

# A unified OLED aging model combining three modeling approaches for extending AMOLED lifetime

Xingtong Jiang, SID Student Member  | Chihao Xu, SID Member

Institute of Microelectronics, Saarland University, Saarbruecken, Germany

## Correspondence

Xingtong Jiang, Institute of Microelectronics, Saarland University, Saarbruecken, Germany.  
Email: xingtong.jiang@lme.uni-saarland.de

## Funding information

German Research Foundation, Grant/Award Number: DFG 282450530

## Abstract

Aging is still the most challenging issue for organic light-emitting diodes (OLEDs), which causes the image-sticking artifacts on active-matrix organic light-emitting diode (AMOLED) displays and limits their lifetime. To overcome this demerit, an aging model is necessary to compensate for aging artifacts. In this paper, we present a unified OLED aging model, which combines three feasible modeling approaches of OLED degradation, namely, data-counting, electro-optical, and correlation methods. The model can be used to predict the efficiency decay of OLED pixels during operation. It mitigates weaknesses and limitations of each of these three models and deploys their strengths, respectively. In the first aging stage, the data-counting model is prioritized, and in the later stages, it is calibrated using the correlation model. The dependency of the efficiency decay on the operation point of OLED is covered by the electro-optical model. The unified model is based on both phenomenal and physical effects. It delivers more reliability to determine an OLED's degradation over a long-term operation and a wide operation range like current amplitude and/or temperature range. The unified aging model applies to either an analog or a digital driving scheme. A corresponding compensation based on the aging model can be applied for extending the AMOLED lifetime.

## KEYWORDS

aging compensation, aging model, AMOLED, correlation, data counting, electro-optical, image sticking, lifetime, OLED degradation

## 1 | INTRODUCTION

Organic light-emitting diodes (OLEDs) have become one of the mainstream display technologies in recent years. They fulfill growing demands for high-quality, flexible, and energy-efficient displays. However, lifetime is still the critical issue for an OLED, hindering its wide

penetration in more application fields, such as automotive or augmented reality (AR).

Image-sticking artifacts (also known as burn-in effect) are commonly observable on active-matrix organic light-emitting diode (AMOLED) displays. This phenomenon is attributed to the OLED degradation. Compared with inorganic light-emitting diodes (LEDs), the OLED is

This is an open access article under the terms of the Creative Commons Attribution-NonCommercial-NoDerivs License, which permits use and distribution in any medium, provided the original work is properly cited, the use is non-commercial and no modifications or adaptations are made.

© 2021 The Authors. *Journal of the Society for Information Display* published by Wiley Periodicals LLC on behalf of Society for Information Display.

more prone to degradation due to instable materials. The luminance output of an OLED decreases gradually with operation time. Image sticking may appear when differential aging occurs among the pixels. Human eyes are sensitive to high-frequency spatial variations. Patterns, which were displayed for a while, may appear unintentionally image sticking. Among the three primary colors, blue suffers the shortest lifetime. Furthermore, aging will be much stronger under higher current operation and/or ambient temperature. These facts make the expectation for a long lifetime display still far away, despite continuous improvements in lifetime issues of OLEDs.

To solve this issue, aging compensation has been considered as a feasible approach.<sup>1</sup> The concept involves compensating the efficiency decay of aged pixels on a matrix. Through evaluation of the efficiency decay and adaption of pixel gray value, the pixel-wise compensation can be executed, and image sticking is then mitigated or eliminated. Lee et al.<sup>2</sup> proposed an external compensation method to alleviate the emission degradation for the AMOLED display. The degradation evaluation through sensing the variation of applied voltage is adopted in the compensation algorithm. It is worth mentioning that the external compensation in general has more potential for solving aging and non-uniformity issues of AMOLED display system than internal method.<sup>3</sup>

However, the actual challenge is the validity and accuracy of an OLED's aging model. An aging compensation is based on an OLED's aging model, which can predict optical decay, because luminance loss in a matrix is not a directly measurable value during the lifespan of a display. In this paper, we are going to present three OLED degradation models. A unified aging model

combining these three modeling approaches is to be developed in order to increase the model accuracy and thus achieve an effective aging compensation.

## 2 | DEGRADATION MECHANISM

An OLED is an electroluminescent organic semiconductor device. When a voltage is applied to it, holes and electrons are injected, transported, form excitons, and finally recombine with emission of light, as shown in Figure 1. The external quantum efficiency (EQE) can be evaluated for light emission. The equation is described as  $EQE = \gamma \cdot \eta_r \cdot q \cdot \eta_{out}$ , where the factor  $\gamma$  is the charge-carrier balance (electron-hole);  $\eta_r$  is the radiative exciton production;  $q$  is the intrinsic radiative quantum efficiency; and  $\eta_{out}$  is the out-coupling factor.

Over a longer period of operation, degradation effects in electrical and optical characteristics may be observed.

### I. Degradation in electrical characteristic

The decay in electrical characteristic is a commonly observed phenomenon, such as the forward-voltage rise<sup>4</sup> or current drift. Considering the current flow generation in a device during the operation process, multiple mechanisms may contribute to this degradation: (i) injection barrier rise originating from interface deterioration, (ii) rising resistance due to trap formation in serial layers,<sup>5</sup> and (iii) accumulation of traps in the emission zone.

### II. Degradation in optical characteristics

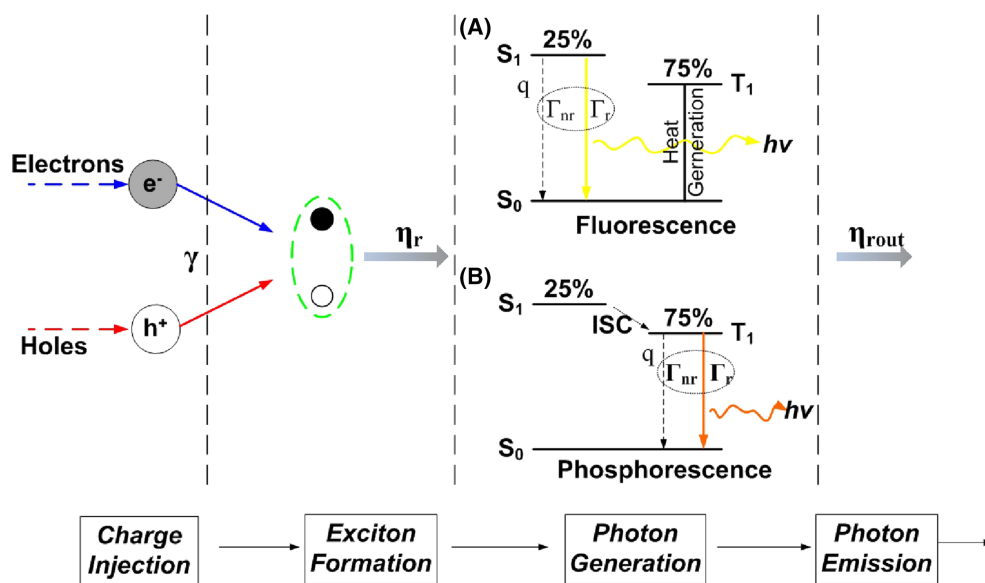


FIGURE 1 Schematic illustration of the light emission process

The decay in optical characteristic is more critical; unfortunately, it is not electrically measured, whereas electrical degradation is. The luminance degrades with operation time, defining the OLED's lifetime. With consideration of the working process and the EQE, the following potential effects may cause degradation: (i) deterioration of charge-carrier balance, (ii) a decrease of radiative quantum efficiency due to creation of trap in emission layer,<sup>6</sup> and (iii) decreasing out-coupling factor.

The electrical and optical degradations not only share some common degradation causes but also have their own degradation causes. Therefore, the correlation between decay in electrical and optical characteristics may be partial.<sup>7</sup> The correlation depends on the aging state, for example, pristine or very aged state, and the operation point also has an influence on the correlation. For the trap formation in emission zone, it may cause the radiative quantum efficiency to decrease and induce an operation voltage rise as well. It is a linked phenomenon from this perspective. Nevertheless, it is incorrect to assume that the luminance efficiency decay and voltage rise have a deterministic relationship.<sup>5</sup> This can be identified with AC aging test, in which AC driving can heal the decay in electrical property but not the decay in current efficiency.<sup>8</sup>

### 3 | ELECTRICAL-OPTICAL DEGRADATION BEHAVIORS

We performed lifetime tests on blue and green OLED devices provided by Novaled and Merck, as shown in Figure 2. The OLED samples were continuously stressed for thousands of hours, and multiple driving conditions (current amplitude and/or temperature) were applied on the OLED devices. The electrical-optical characteristics and their degradation behaviors were measured and analyzed during the lifetime tests. While increasing the applied voltage, the OLEDs experienced various regimes. In addition, with aging time, the electrical (I-V) and

optical characteristics (Eff-V) dramatically decayed, as shown in Figure 3. At a given operation voltage, the current flow gradually drops. Simultaneously, the current efficiency declines with aging time. OLEDs are vulnerable to operational degradation. Furthermore, it was discovered that the current efficiency decay depends on the operation points.<sup>9</sup> For example, the current efficiency decay at 2.6 V is much stronger than at 3.5 V after 2000 h of operation. This means that the efficiency decay is not only a function of operation time but also a function of operation point. Besides degradation behaviors in electro-optical characteristics, some potential impact factors on degradation behaviors were also investigated. It was observed that the efficiency decay depends on driving conditions, including current amplitude and temperature. They exert an acceleration effect on the degradation behaviors. These facts should be considered in an OLED's aging model. It is worth noting that the blue fluorescent and green phosphorescent OLEDs show similar degradation behaviors in aging process.

The idea of compensation of OLED aging by adapting pixel gray value might be straightforward. However, the efficiency decay of aged pixel cannot be measured, when an OLED-equipped device is with the end-user. The key is a proper OLED aging model determining the efficiency decay without any optical measurement.

### 4 | MODELING OF OLED DEGRADATION

To effectively compensate pixel-wise luminance loss, which induces the image-sticking artifacts on AMOLED displays, modeling the degradation behavior of an OLED is necessary. Because of limited understanding and complex dependency of degradation mechanisms, it is not practical to build a comprehensive physical model for an OLED degradation. In this paper, three feasible degradation modeling approaches are presented for aging compensation.<sup>7,10,11</sup>

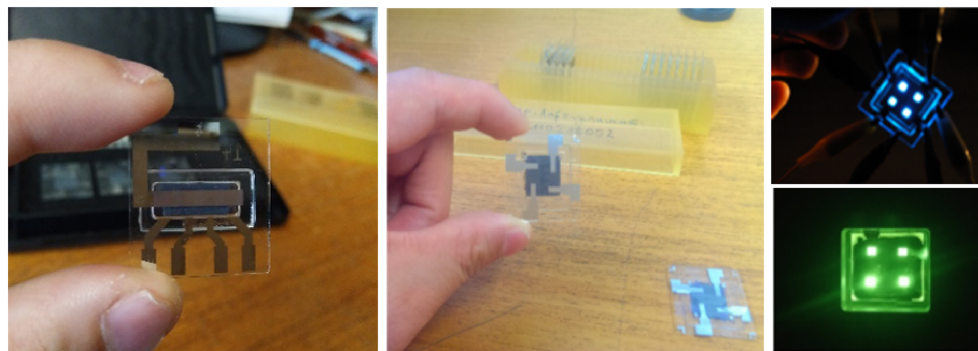


FIGURE 2 OLED devices for lifetime test (Novaled, Merck)

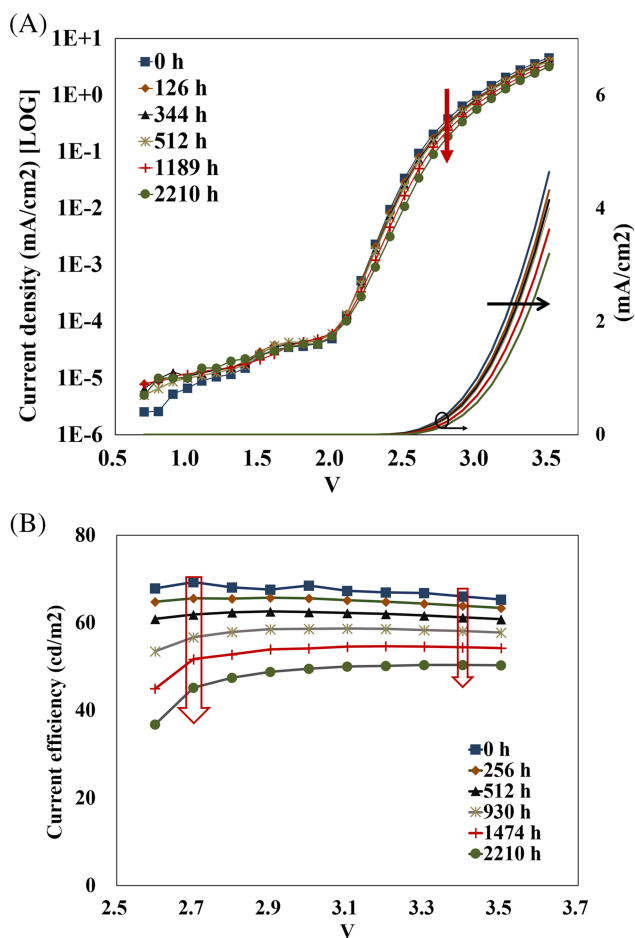


FIGURE 3 Current-voltage ( $I$ - $V$ ) curves (A); current efficiency versus voltage ( $Eff$ - $V$ ) curves in aging (B). Data from Merck green phosphorescent OLED devices

#### 4.1 | Data-counting model

A data-counting model has been proposed as a pragmatic mean to predict aging in operation.<sup>10</sup> The empirical model considers the OLED decay under multiple driving conditions, namely, various current amplitudes and ambient temperatures. Through calculation of accumulated stress on devices during operation, the decay could be evaluated. A unified decay profile is derived by integrating multiple decay curves under various driving conditions—this may meet practical conditions in most applications.

During operation, the current efficiency of an OLED gradually decays. With consideration of driving conditions, the degradation can be described as a function of three impact factors, namely, the current amplitude  $I$ , temperature  $T$ , and the operation time. Equation 1 describes the accumulation stress  $Acc$  on an OLED in the aging process, based on the coulombic degradation law,<sup>12,13</sup> the current amplitude, and thermal acceleration

effects.<sup>13,14</sup> The coulombic law interprets that a total amount of injected charges into an OLED quantifies the decay of current efficiency. The acceleration factor for current amplitude and temperature is formed in this equation, which is derived from experimental observations. A unified decay profile for current efficiency is derived as shown in Equation 2. The current efficiency  $\eta$  is normalized to 1. Here,  $\alpha$  is the decay exponent.  $Q_{80}$  is defined as the accumulation quantity of injected charges, when the current efficiency decays to 80% of its initial value. This parameter depends on the current amplitude and temperature (given reference points  $I_{ref}$  and  $T_{ref}$ ). The quantity of 80% is a reasonable value to specify the lifetime for most applications.  $Q$  is the injected charge during operation and mathematically the temporal integration of the OLED current. In an OLED display system, it is proportional to the gray values (GV) accumulated, which have been displayed on a pixel. Thus, this method is called data counting.

$$Acc(I, T) = \int \left[ \left( \frac{I}{I_{ref}} \right)^{\beta-1} \cdot \exp \left( \frac{E_a}{k_B T_{ref}} - \frac{E_a}{k_B T} \right) \right] \cdot I \cdot dt \quad (1)$$

$$\eta = \frac{1}{1 + 0.25 \times \left( \frac{Acc(I, T)}{Q_{80|I_{ref}, T_{ref}}} \right)^\alpha} \quad (2)$$

Figure 4 shows the unification of multiple decay curves to single decay profile for multiple driving conditions. Figure 4A is the measured multiple decay curves during lifetime tests with operation time on the  $x$  axis. Figure 4B displays a modeled unified decay profile considering coulombic degradation, current amplitude, and thermal acceleration effect with  $ACC$  (Equation 1) on the  $x$  axis. By counting the accumulation stress on the device, the data-counting model with unified decay profile can predict the OLED degradation under multiple driving conditions. Based on such a model, the pixel-wise compensation can be implemented for an AMOLED display in real operations with varying current amplitude and temperature.

Nevertheless, errors in model parameters, current, and temperature may be accumulated. In the long term, there may be a significant accumulation error for predicting the relative efficiency, resulting in a lower quality of compensation. Moreover, the current efficiency decay also depends on operation point; thus, several decay profiles may be needed in a display system. This would not be an issue for the digital driving scheme due to a fixed operation point but would be an issue in an analog driving system. Equation 2 delivers a relative efficiency value, which is valid for one operation point, for

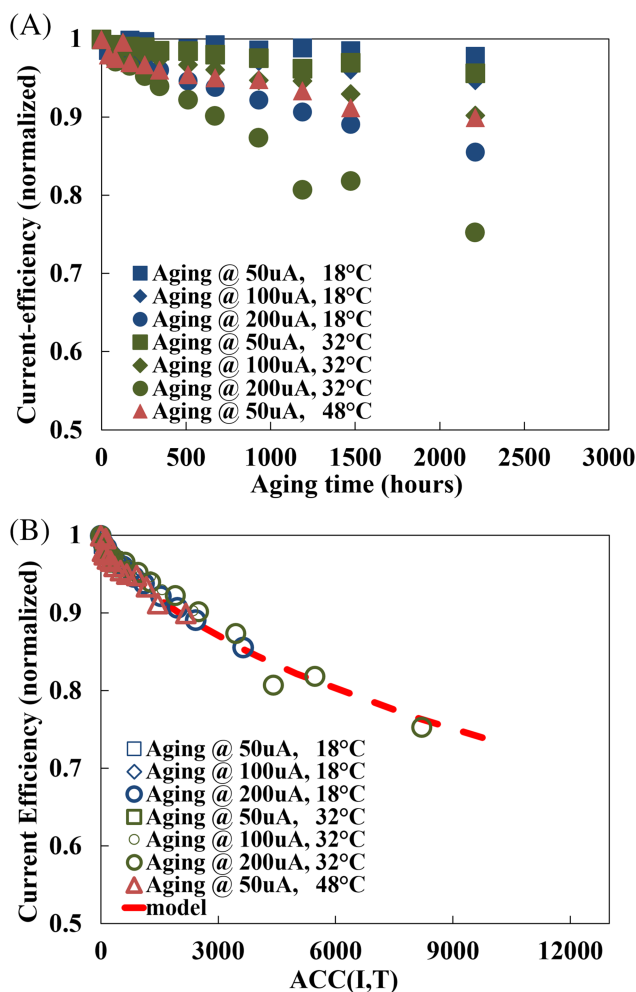


FIGURE 4 Measured multiple decay curves (A) and modeled unified decay profile (B) for OLED driven under various conditions

example, a defined current. The dependence over a wide current range may be covered by an electro-optical model.

## 4.2 | Electro-optical model

To simulate the efficiency decay with dependency on an operation point, an electro-optical model has been developed.<sup>11</sup> An OLED device generally contains several organic layers, namely, injection layers (holes and electrons), transport layers, and the emission layer. Electrically, it can be described as an equivalent circuit of multiple diodes and resistors, as shown in Figure 5.

Two or more serial diodes (e.g., EIL-ETLHIL-HTL) are merged into one serial diode  $D_{ser}$ . The OLED device has a resistance in each layer, which is summed up to the resistance  $R$ . For the emission layer, it is modeled by three elements, namely,  $D_{emit}$ ,  $D_{non}$ , and  $R_{leak}$ . In the emissive layer, OLED current is split into three branches, as the equation  $I_{OLED} = I_{leak} + I_{emit} + I_{non}$  shows.

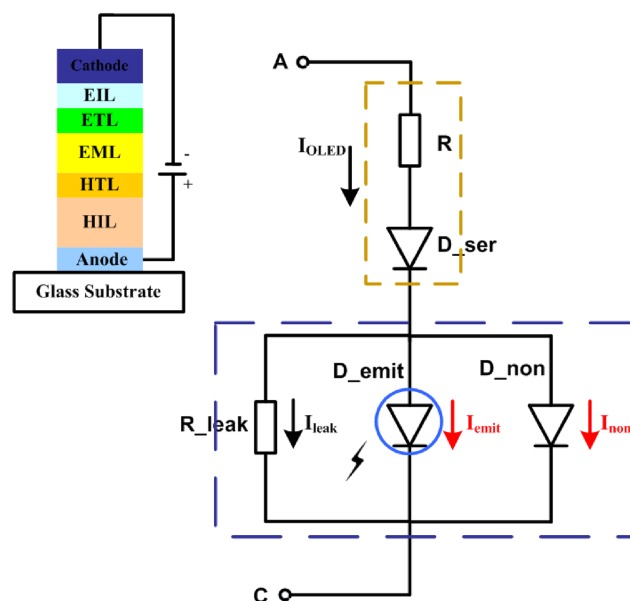


FIGURE 5 Structure and equivalent circuit of an OLED device

The leakage current is modeled by the leakage resistor, of which the influence will disappear, if either  $D_{emit}$  or  $D_{non}$  starts to conduct. The current flowing through  $D_{emit}$  ( $I_{emit}$ ) generates visible light, whereas non-emissive current ( $I_{non}$ ) flows through  $D_{non}$  without generation of any light, which is attributed to the fact that the electron-hole pair annihilates in form of radiative and non-radiative recombination. The intrinsic radiative efficiency  $\eta_{int}$  as the property of  $D_{emit}$  (ratio between the luminance and  $I_{emit}$ ) is assumed to be constant in the operation of the model. The current efficiency  $eff$  for an entire device is thus described as the equation  $eff = I_{emit}/I_{OLED} \times \eta_{int}$ . The formula indicates that the current flow distribution causes the operational dependency of current efficiency.<sup>11</sup> This is valid for any aging state. Consequently, the current efficiency depends on operation point, as observed in the experiments.

Based on the equivalent circuit, the electrical and electro-optical characteristics in dependency on operation point can be simulated, as shown in Figure 6. At low operation point, the device enters a leakage region. One kind charge (hole) is solely injected into the device and accumulated at the interface, whereas a small portion of holes will reach the cathode, forming a leakage current flow through device. In the model, the low leakage region is dominated by  $R_{leak}$ , related to a leakage current. Due to the absence of electrons, the OLED device is dark, and the efficiency is 0 in this operation region. In the following middle operation range, the device enters a recombination region, and current efficiency climbs significantly. The electrons are injected into the organic layers, with an improvement of charge balance. The recombination flow

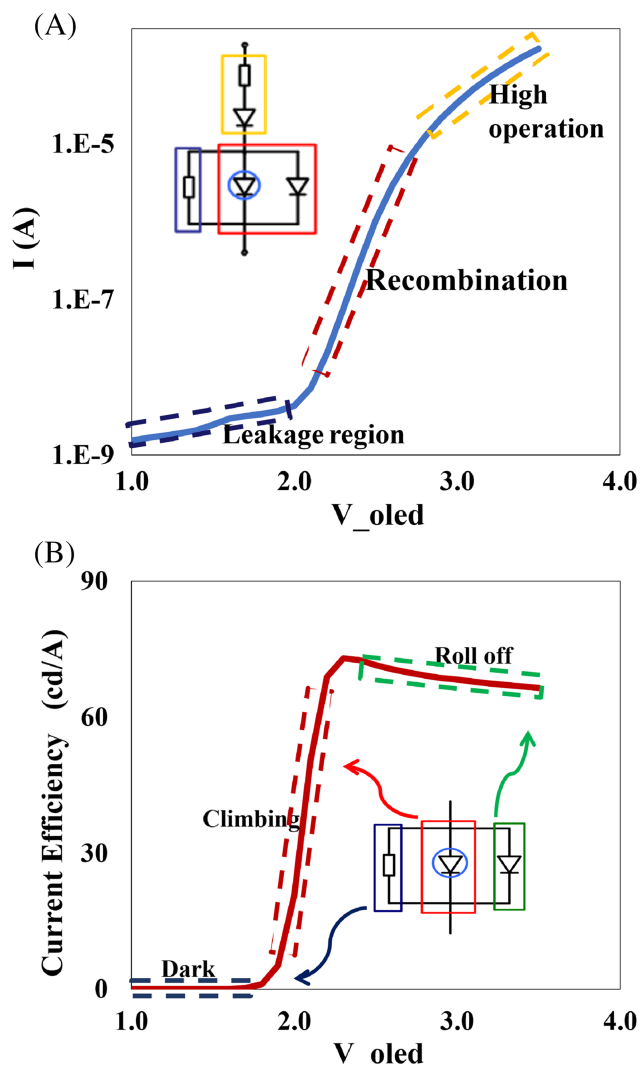


FIGURE 6 Electro-optical characteristics: Current-voltage curve (A); current efficiency versus voltage curve (B)

is a twofold: the radiative recombination that generates photons and the non-radiative recombination that does not emit visible light. In the model of Figure 5, the  $D_{emit}$  and  $D_{non}$  denote the emitting and non-emitting path, respectively. Both diodes have different parameters. The leakage path becomes a negligible share. In the high operation range, there is a rectification effect for the current flow, which refers to non-ohmic and ohmic conduction in/between multiple serial layers. And a roll-off effect dominates the optical behaviors. It may be attributed to the lack of charge balance or exciton quenching.<sup>15</sup> In the model, the serial diode and resistance cause an electrical rectification behavior, and non-emission diode influences the optical behavior in the high operation range. The non-emitting diode has a lower emission coefficient than the emitting diode; thus, the current efficiency declines.

This electro-optical model is valid through the entire lifespan of an OLED, as the physical structure stays unaltered. In the aging process, the electrical and electro-optical characteristics gradually degrade, as shown in Figure 7. The degradation behaviors in the electrical and optical properties due to internal degradation mechanism can be modeled by the drifting parameters in the equivalent circuit. The deteriorated interface or formed traps in serial layer may result in a degradation behavior in current-voltage ( $I$ - $V$ ) curves (Figure 7A). The drift in rectification region can be modeled by varying the parameters of the serial diode and/or resistance. The degradation mechanisms, such as decreasing radiative quantum efficiency due to traps creation in emission layer,<sup>6</sup> may induce a degradation behavior in current efficiency ( $Eff$ - $V$ ) curve (Figure 7B). Based on the equivalent circuit, the degradation behavior is interpreted by the aging on the emitting diode, particularly the decreasing saturation current of the  $D_{emit}$  model. At a very low voltage, the fitting shows a deviation to some extent. There may be

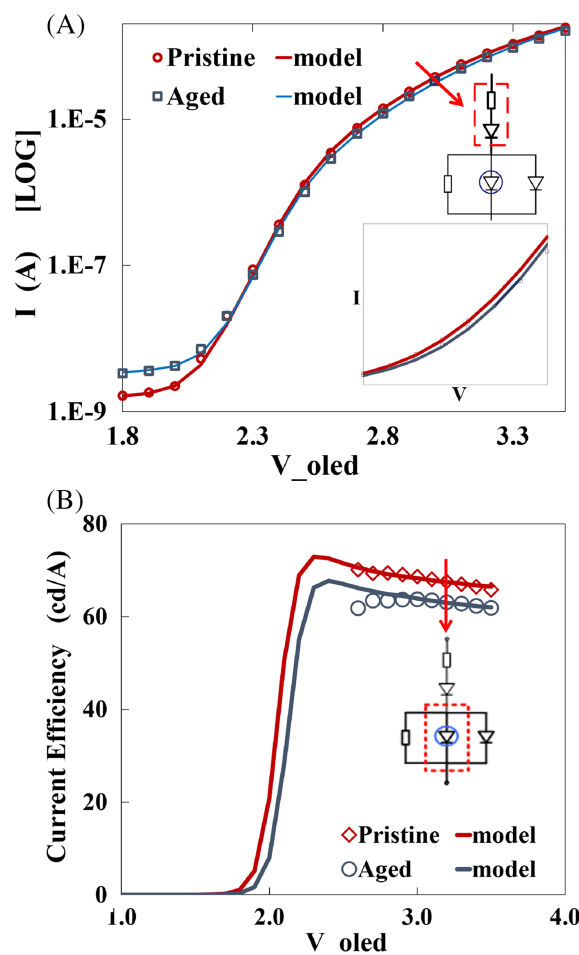


FIGURE 7 Measured and simulated (solid lines) electrical-optical characteristics in aging: Current-voltage curves (A); current efficiency versus voltage curves (B)

two roots: very simple model for the leakage path; and measurement error due to very low current and particularly low luminance. Because OLEDs are generally operated at a range where recombination current is more predominant, a certain discrepancy at low voltages need not to be solved.

The model parameters of the equivalent circuit drift during aging process; thus, the current distribution ( $I_{emit}/I_{oled}$ ) drifts as well, resulting in the decay of the current efficiency. An effective approach is to model the drift of parameters. For a stringent parameter extraction and clear interpretation, a few model parameters may drift with the operation time. The drifting parameters should show a reasonable trend that is consistent with electro-optical decay behaviors<sup>11</sup> and can be explained by physical degradation phenomena.

### 4.3 | Correlation model

Besides the two modeling approaches above that are not competing but rather complementing, an additional feasible approach to quantitatively evaluate the efficiency decay is to be introduced, namely, the correlation model. This method is intended to derive a correlation between optical decay and measurable electrical value. In contrast to the data-counting model that is a look-forward method, the correlation is rather a feedback approach. An issue like error accumulation inherent in a data-counting model no longer exists. Chen et al. proposed a capacitance-based method for degradation.<sup>16</sup> However, the approach using capacitance as an indicator for optical decay is not promising. The capacitance hardly drifts in our lifetime tests, so that its sensitivity has been concluded as low. A different approach is to measure the voltage rise at a constant current for estimation of the efficiency decay.<sup>17</sup> But sensitivity is in this case low as well due to a modest variation during aging process, as the voltage is a logarithmic function of current. The opposite measurement, measuring current at a constant voltage, is much more sensitive, and it fits well to a digital driving scheme. Thus, current measurement has been chosen to evaluate the efficiency decay.

A correlation between the current efficiency decay and current drift in aging process is plotted in Figure 8. It identifies that the decay in electrical and optical characteristics may be fundamentally linked phenomenon according to the analysis of degradation mechanism.

The pixel current is thus a sensitive measurable value to derive the efficiency decay based on the correlation profile. A linear correlation between relative efficiency drift and relative current drift had been proposed for aging compensation by our group.<sup>18</sup> It is worth

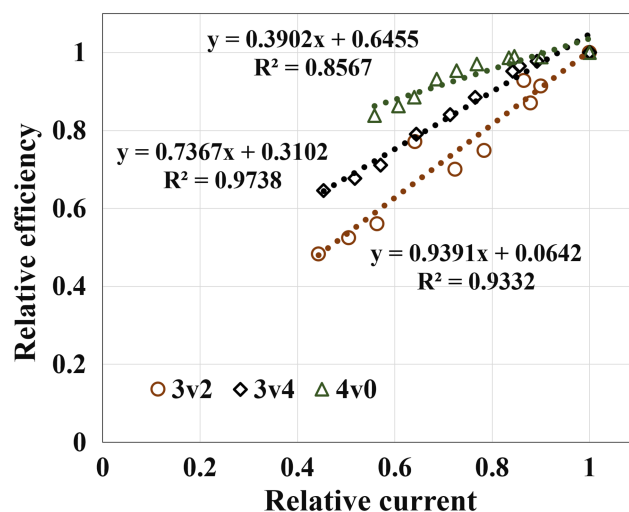


FIGURE 8 Correlation of efficiency decay and current drift in experiment and simple linear correlation profile

mentioning that the relative current efficiency is of particular benefit, as it can directly be used for the aging compensation, as will be described in Section 5.3. The relative current efficiency is referred to as relative efficiency in this paper. The following formula may be formed to approximate the correlation:

$$\frac{\eta}{\eta_{pristine}} = k \times \frac{I}{I_{pristine}} + d \quad (3)$$

$k$  is the proportional factor, and  $d$  is offset. Both depend on the operation voltage. The offset may be ascribed to the rising of serial resistance or interface deterioration in the OLEDs during the beginning phase of aging. In Figure 8, the correlations of efficiency decay and current drift at three operation points were fitted with a linear formula. Parameters for Equation 3 have been extracted from measurement data for these three operation voltages and stated in the plot.

Even though there is a strong relation between efficiency decay and current drift, the correlation is not 100%. Indeed, the decays in electrical and optical characteristics are partially correlated. Some degradation mechanisms may contribute to both, whereas others may only impact one of them. As mentioned before, the deteriorations of injection interface and charge transport cause decay in the electrical characteristic, whereas the accumulation of charge trap in EML may induce both voltage rise and current efficiency decrease. Thus, a correlation model based on accumulation of charge trap in EML is expedient. Figure 8 shows that the slopes increase at a lower operation voltage. Figure 9 also shows that the correlation depends on the operation point. The curve at a lower voltage point (i.e., 3.2 V) is well fitted with the

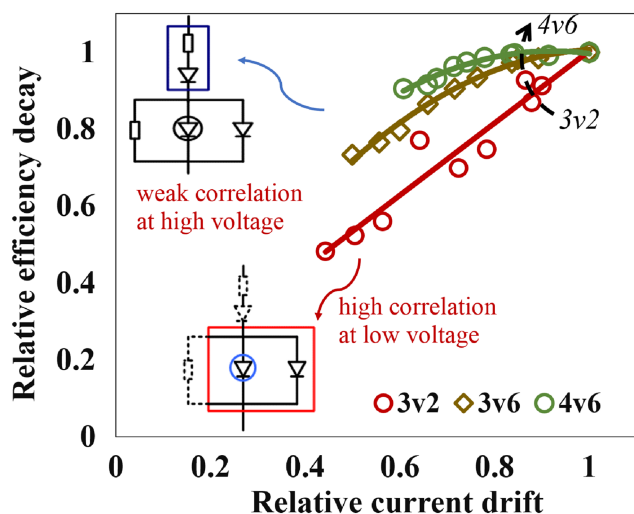


FIGURE 9 Correlation between the efficiency decay and current drift at three operation points

linear formula, whereas the curves at higher points depict less fitting. At the high-voltage point, the current drifts more sharply than efficiency decays, especially in the beginning phase of aging. It implies that the correlation at higher operation point is weaker compared with the lower operation points. Based on the equivalent circuit, the partial correlation of electrical and optical decay can be analyzed and identified. The serial elements (serial resistance and diode) and parallel elements (radiative, non-radiative, and leakage) have impact on the I-V characteristic. For the optical characteristic, the current efficiency is determined by parallel elements (internal current flow distribution between  $D_{emit}$  and  $D_{non}$ ). At higher operation points, the serial layers exert a significant rectification on current flow. The deterioration of serial elements then plays a much stronger role in current drift, beside the drift caused by the parallel elements. The current drift is therefore just partially correlated with the efficiency decay. At a lower voltage point (3.2 V), there is a nearly full correlation between current drift and efficiency decay. It means both current drift and efficiency decay are attributed to the same deterioration in parallel elements (EML).

The correlation model allows also an insight into the location and time of degradation effects. The serial elements have impact on electrical characteristic, but not on optical characteristic. Among them, the degraded serial resistance has no impact in the low operation range, where the current is very low and does not cause any real voltage drop across a resistor. If the operation voltage is high, the degraded serial resistance would interfere with the I-V, thus partial/lower correlation. The degraded serial diode will have an impact in the low operation

range (3.2 V) as well as in the high operation range (4.6 V). The fact that the correlation in the lower operation range is nearly 100% may yield to the conclusion that the serial diode no longer drifts, after a very short aging time has passed, although the serial resistance drifts in long-term operation. The accumulation of traps in the emission zone causes decay of electrical current and the mostly undesired effect, current efficiency decay. This effect can be correlated to electrical current decay. Beyond the findings above, the original scope of the correlation model remains; it shall be applied for aging compensation, as will be described afterwards.

The degradation of an OLED is substantially influenced by driving conditions such as luminance level or ambient temperature. The electrical and optical characteristics do not always decay hand in hand due to partial correlation, as analyzed above. The correlation curve may deviate from a linear function, especially in higher operation points. However, in lower operation range, the current drift and efficiency decay share identical degradation mechanism and deterioration of radiative diode. Therefore, the two decays are synchronous, and the correlation exhibits a linear profile. Because of the identical cause of both decays at a lower operation point, the correlation does not alter with various driving conditions, but as one single unified profile. This is depicted by Figure 10 showing the unified decay correlation profile at lower operation point for devices stressed under various driving conditions. This unified correlation profile may prove that the model is valid over a wider operation and temperature range.

The correlation model aims to derive the efficiency decay with the measurable electrical value. However, the

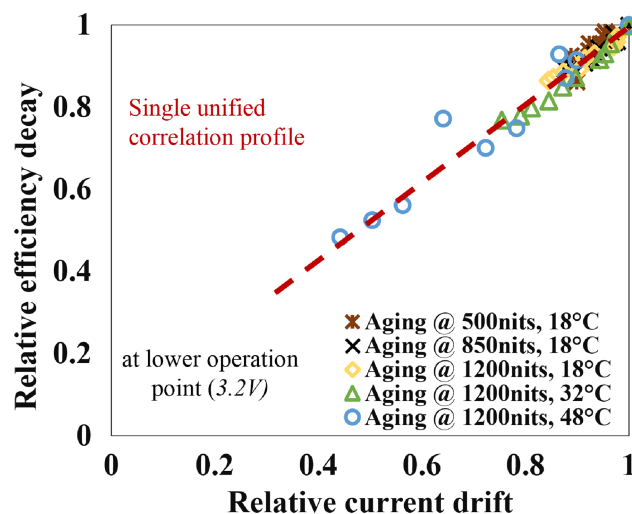


FIGURE 10 Unified decay correlation for various driving conditions



correlation between efficiency decay and current drift depends on operation point. In higher operation voltages, the correlation is partial and thus not reliable. The challenge is how to evaluate efficiency decay at a higher operation point, which is of more concern in real applications. To solve this problem, the correlation model may be combined with the equivalent circuit. The correlation is high at a low operation point and can be chosen to determine the aging parameters in the equivalent circuit and derive the efficiency decay at higher operation points. An efficiency decay in a wide operation range can thus be evaluated with correlation and the equivalent circuit. Compared with the data-counting model, the correlation model may prevent the error accumulation in the long-term operation and deliver more reliable results in a strongly aged state.

## 5 | UNIFIED AGING MODEL FOR AMOLEDs

In the previous sections, three models were presented, providing the potential and feasible approach to predict the degradation in quantity. However, they have their own strengths and weakness. For the data-counting model, the accumulation stress is counted, and the efficiency decay is evaluated from a decay profile. In the long term, errors in parameters, current, temperature, and so forth may be accumulated; thus, deviations may get larger and larger with time. In comparison with the data-counting model, the correlation model delivers evaluation of the efficiency decay with measurable electrical value, seen as a feedback approach. It can overcome the issue of error accumulation in the data-counting model and deliver more reliable results in a strongly aged state, despite the fact that this model shows more deviation in the initial decay process. One example is that an offset value is needed in Equation 3. In addition, the decay after an electrical measurement cannot be tracked, so thus, the efficiency decay may look stair-like. The real value of the electro-optical model is that the electrical-optical performance in a wide operation range can be quantitatively derived, by considering the internal current distribution in the equivalent circuit. The dependency on operation point for efficiency decay can be described and determined. Therefore, a unified aging model combining these three approaches may deliver more reliability and effectiveness to accurately model the OLED degradation. The corresponding compensation in driving system can thus be applied to suppress image-sticking artifacts on an AMOLED display. This section describes the combination of the three models and its application in aging compensation. It contains the following parts:

Section 5.1—aging calculation for a long term; and Section 5.2—aging calculation for an operation range. Besides the unified aging model, the aging compensation for an AMOLED system will be presented in Section 5.3.

### 5.1 | Calibrated aging calculation for a long term

The data-counting model is a looking-forward method, of which the quality may be increased, if it is occasionally calibrated during the whole lifespan. The correlation model is a feedback method that may calibrate the data-counting model. Both models state a relative efficiency for an operation point. The data-counting model may be established by tests at a medium and high operation point, so that the lifetime test is not extremely long and has application-like conditions. On the other hand, the correlation model has a high correlation at a low or medium operation point. Thus, a medium operation point shall be chosen for the combination of both models. The relative efficiency for a defined (medium) operation point is termed in this paper as aging status. The equivalent circuit model can take the aging status value and deliver a relative efficiency value in dependence on the real operation point given by the display application.

To achieve long lifetime, the relative efficiency should be accurately predicted in a long-term operation. The data-counting and correlation approach can be combined in the aging model with dependence on the aging status. A combination is shown in Figure 11. The relative efficiency shall represent the aging status. Two aging phases are defined. First is the beginning phase, which is a rapid aging period. In this initial period, the relative efficiency may not correlate well with the relative current, as described above. The data-counting method is solely

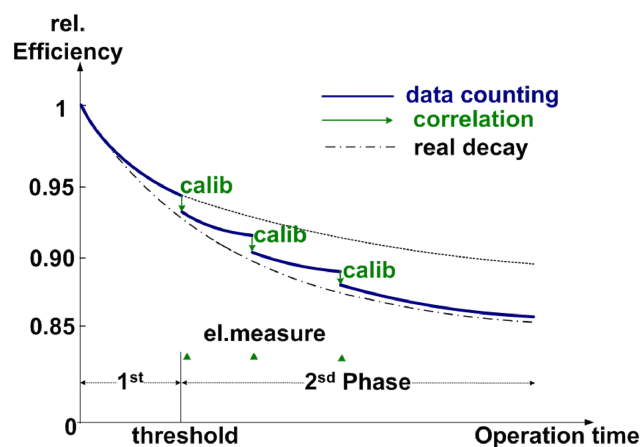


FIGURE 11 Combined models for a long-term operation

applied. Because the duration of this period is relatively short, the error accumulation is limited and the model accurate. The second phase is a much longer aging period with much slower, but stronger decay. In this period, the correlation approach is applied and combined with data counting in the aging calculation. The electrical measure method can deliver more reliable results in a strongly aged state than the data-counting model. It is executed after certain periods of aging time. The interval (duration) between two measurements may get longer, when the OLED has been stressed for a longer period of time or a higher current amplitude/temperature. The deviation of aging calculation due to accumulated error in previous state can be gradually calibrated. The evaluated efficiency decay may be finally close to real decay value and more accurate than each of the data-counting model and the correlation model alone.

Figure 11 shows an exemplary procedure for the combination. The blue solid line is the data-counting approach with declining efficiency over operation time. The green triangles indicate the time of electrical measurements, and the green arrow lines denote the calibration steps. The formula and procedure for the calibration will be described mathematically later in this section. The combination of these two approaches describes a practical aging calculation path over the whole operation period, of which the relative efficiency shall be close to the real decay profile. If only the data-counting model is applied (dotted line), the aging prediction will significantly deviate from the real decay, as shown by the dashed line in this figure. The electrical measurement should be triggered at a reasonable interval, satisfying the tolerance of the human eyes (e.g., the relative change is less than 1%).

Additionally, the threshold may be defined by the deviation between electrical and optical decay in the correlation model during the beginning of operation. In the initial aging phase, the OLED device is more vulnerable to a deterioration of serial layers and/or interfaces, resulting in strong decay in the electrical property but not as much in the optical performance. The current drift has an offset of about 5% for the case of Figure 8 at 3.2 V. The  $d$  parameter in Equation 3 is 0.06. Therefore, a threshold of 0.95 is reasonable. Due to the asynchronous electrical and optical decay, the correlation approach is not applied in the beginning phase. Because the operation time of this phase is short, it can be expected that the error accumulation of the data-counting model is low. Thus, the data-counting model is solely applied in the first phase.

In the second phase, degradation occurs in the emission layer and serial layers (trap formation). If the electrical current is low, a good correlation between decay of

electrical current and decay of the current efficiency can be assumed. Thus, the correlation model will have a higher weight in the combined model, which will be described by a formula later. This means that the data-counting model and the correlation model are combined. The exact procedure will be described in the next paragraphs. The plot in Figure 11 is firstly explained. When an electrical measurement has been performed, the correlation model will deliver a relative efficiency value, which is to be combined with the data-counting model. The correlation model may calibrate the data-counting model including the ACC value. Before the next electrical measurement, the data-counting model can further calculate the relative efficiency online, so that the relative efficiency continues to fall gradually. This process is depicted in Figure 11 by the falling edge after each calibration and decreasing curve between the two calibrations.

Figure 12 shows a procedure for the aging model combining the data-counting model and the correlation model for a long-term aging process. In this diagram, the aging status is calculated by weighting the evaluation from both approaches. The weight factor is a function of the aging status. The data counting is real-time operation during the whole lifespan, whereas the correlation applies for aging calculation at intervals along the second aging phase. In the long-term aging period, the calibration will be executed intermittently after each measurement until the end of the lifespan. The output, aging status flows into a procedure of calculation for a wide operation range and aging compensation, as will be described later in this section.

Figure 12 is described here in detail. The data-counting model provides a method for quantitatively predicting the OLED's aging during operation, as described in Section 4.1. In this model, the input image data and driving conditions are accounted for each pixel during operation. The driving conditions consider current amplitude and ambient temperature as the aging acceleration factors. Based on the record of driving history, the stress accumulated can be calculated for each pixel. This function is accomplished in module of ACC in diagram, and the formula refers to Equation 1 in Section 4.1. After determining the accumulated stress, the decay in current efficiency can be derived from a unified decay prediction profile (UDP). It refers to the formula, that is, Equation 2. Multiple driving conditions are considered in the calculation. The model's parameters may be extracted from a sample set of device samples in previous aging tests. Take the following procedural as an example. At each time point ( $0-t_1-t_2 \dots$ ), the accumulation stress  $Acc$  in the operation period is calculated, and the relative efficiency at each point ( $1-\eta_1-\eta_2 \dots$ ) can be then derived.

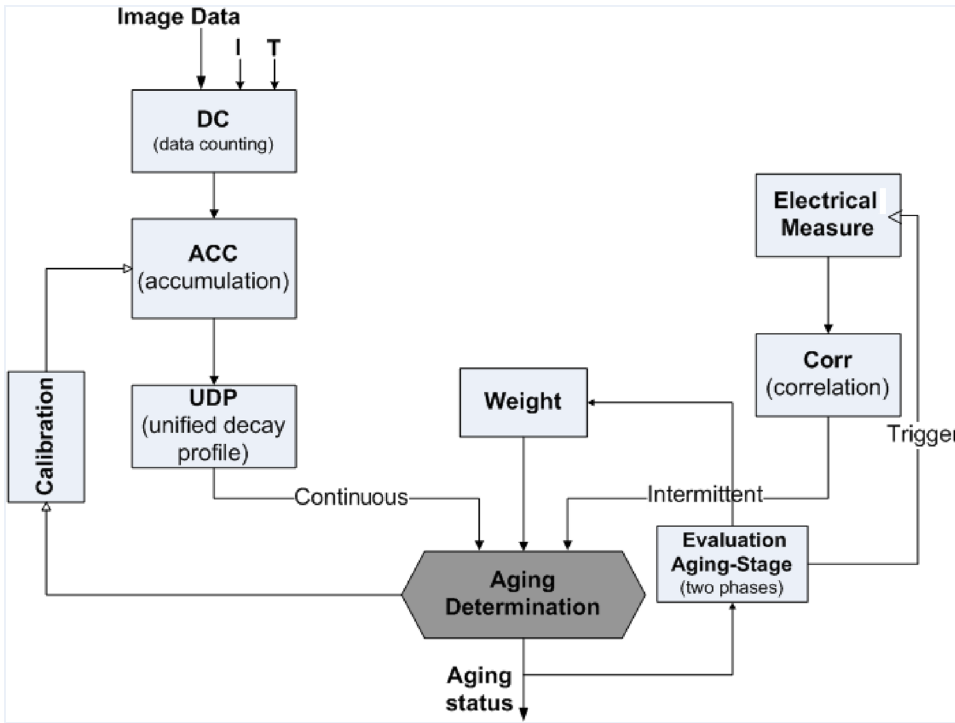


FIGURE 12 Diagram for combination of data-counting and correlation methods for a long operation term

$$0: Acc_{t_0} = 0 \quad \eta_{t_0} = \eta_{pristine} = 1$$

$$t_1: Acc_{t_1} = Acc_{t_0} + \int_0^{t_1} f(I(t), T) \cdot dt, \eta_{t_1} = \frac{1}{1 + 0.25 \times \left( \frac{Acc_{t_1}}{Q_{80|I_{ref}, T_{ref}}} \right)^\alpha \dots}$$

(4)

In the second aging phase, the correlation model is applied for calculating the aging status. The correlation model can derive the optical decay with a measurable electrical value. The correlation of efficiency decay and current drift was identified and modeled, as described in Section 4.3. In the aging model, the electrical measures will be used to evaluate the current drift of pixels and its distribution on panel matrix. According to the correlation between electrical and optical decay, the relative efficiency can be determined. This function is executed in the block of Corr in Figure 12. Electrical measurements can be triggered by auto or manually setting in a display system (e.g., measure at each time before turning on the display). Due to the partial correlation of electrical-optical decay, the current drift measure may be taken at a low or medium operation point (OP) for a higher correlation. The combination of the data-counting model and the correlation model should deliver a degradation value, for example, relative efficiency at one defined operation point or an aging parameter of the equivalent circuit model. The usage of electro-optical model for further OPs will be discussed in Section 5.2.

The two relative efficiency values from both models will flow into *Aging Determination* block (Figure 12). In

this block, the aging status will be calculated taking into account efficiency decay of both data counting and correlation, and the weight factor according to aging stage. The calculation is as shown in Equation 5.

$$\eta_{STATUS} = W_{DC} \cdot \eta_{DC} + W_{CORR} \cdot \eta_{CORR} \quad (5)$$

The weight factor  $W_{DC}$  and  $W_{CORR}$  are one in sum. In the first aging phase, the weight factor  $W_{DC}$  is 1 because data counting is solely applied for calculating the efficiency decay. In the second aging phase, the correlation evaluation is combined into aging calculation, with a gradual higher weight factor preferred. The weight factors are determined by the aging stage of the whole period. The function may be described as the following formula:

$$W_{DC} = 1 - W_{CORR} = f(AgingStatus) = f(\eta_{STATUS}) \quad (6)$$

Aging status may be the relative efficiency and noted as  $\eta_{STATUS}$ . Because the aging is a slow process, the last aging status may be used as in Equation 6. An exemplary curve of weight factors with dependency on aging status in the long term is as shown in Figure 13. The module “evaluation aging stage” determines the weight factors and triggers electrical measure at intervals.

By combining both modeling approaches in the aging model, the aging status can be effectively and dependably determined during the whole operation period. Possible random faults of the two models may get mitigated.

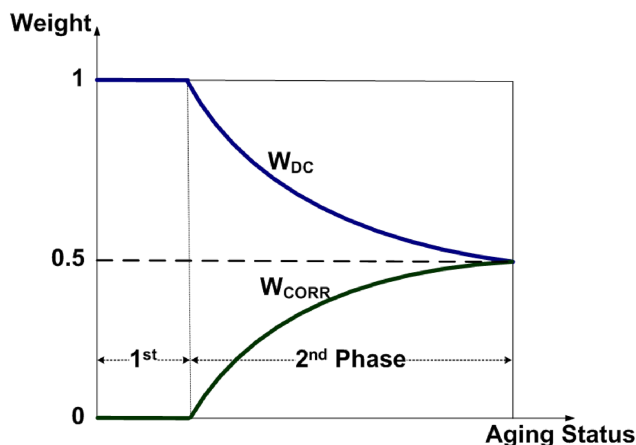


FIGURE 13 The two weight factors during aging

Using the feedback electrical method, the off-track accumulation stress by data counting can be calibrated as well, according to weighted aging status. To further use previously calibrated value in the data-counting procedure, the formula (Equation 7) is applied. The formula is a reverse function of Equation 2.

$$Acc = g'(\eta_{STATUS}) = Q_{80} \cdot \left[ 4 \cdot \left( \frac{1}{\eta_{STATUS}} - 1 \right) \right]^{\alpha^{-1}} \quad (7)$$

The calibrated value will be used to further accumulate new stresses by using Equation 4, whereby the output of Equation 7 is the starting value. This way, the accumulation stress can be calibrated, so that the data-counting model may deliver a continuous and consistent value. Based on this, the relative efficiency can be calculated as the slowly falling curves depicted in Figure 11. The results can be stored in memory, which may be used for aging compensation, as will be described in Section 5.3. The data-counting and correlation methods are complementary. A regular calibration of the data-counting model by the correlation model may make the calculation of aging status more accurate and closer to the real decay. The data-counting model will be evaluated online. The overall deviation of this combination can be closer to the lower one of these two models.

## 5.2 | Relative efficiency in dependence on operation point

The OLED decay depends on operation point, as discussed in the degradation behaviors from experiments in Section 3 and shown in Figure 3. The efficiency decay may depend on operation point. As seen in Figure 3B,

the decay of current efficiency at a lower operation point is much stronger than at a higher operation point, particularly at a strongly aged state. This is the dependency that is more relevant in an analog driving scheme especially in a wide operation range. The aging status or the relative efficiency as delivered by the combined model of data counting and correlation is only valid for an operation current, and it does not directly apply for an operation range. To effectively evaluate/derive the efficiency decay in an operation range, the electro-optical model is to be integrated into the unified aging model.

The electro-optical model is built based on an equivalent circuit. It can merge electro-optical behaviors. The link between photon flux and electrical current is the constant intrinsic current efficiency  $\eta_{int}$  of the diode  $D_{emit}$ . This efficiency is modeled as a constant over both the whole current range and the whole lifespan. Degraded model parameters can describe the decay of electrical and thus optical properties and current efficiency during the entire lifespan. The most important drifting parameter is the saturation current  $I_{S_{emit}}$ , which declines with the operation time.<sup>11</sup> Through determination of the drifting parameters in the equivalent circuit, the corresponding efficiency decay for an operation point, for example, given by image data, can be derived. Figure 14 maps an OLED pixel as a gray box with essential currents and photon flux. This circuit of three diodes and two resistors shall represent the structure of an OLED.

When a voltage is applied, current will flow through the OLED device. The light emitted is the real output, which is a function of the internal radiative current flow ( $I_{emit}$ ), the product of  $I_{emit}$ , and the internal efficiency

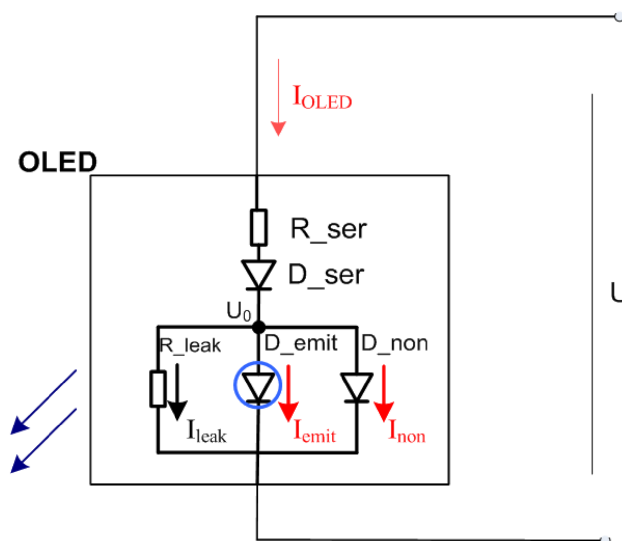


FIGURE 14 OLED as gray-box device in operation

( $\eta_{int}$ ). The current efficiency in dependence on the  $I_{oled}$  is determined by internal current distribution in device. The relevant part of the equivalent circuit (Figure 14) for current efficiency is described by the following formulas.

$$I_{OLED} = I_{leak} + I_{emit} + I_{non} \approx I_{emit} + I_{non} \quad (8)$$

$$I_{emit} = I_{Semit} \left[ \exp^{\frac{U_0}{n_{emit} \cdot V_T}} - 1 \right] \quad (9)$$

$$I_{non} = I_{Snon} \left[ \exp^{\frac{U_0}{n_{non} \cdot V_T}} - 1 \right] \quad (10)$$

Because the parameter  $I_{Semit}$  decreases with operation time, the voltage across the internal diode voltage  $U_0$  increases for a constant current  $I_{oled}$ . At a low  $I_{oled}$ , the drift of the serial resistance does not matter as described in Section 4.3.

The aging process of an OLED is mapped by drifting parameters of the model. The primary aging parameter, the saturation current of  $D_{emit}$ ,  $I_{Semit}$  is responsible for efficiency decay and current drift. The serial resistance  $R_{ser}$  contributes to the decay in electrical characteristic (current drift). It is worth noting that  $I_{OLED}$ , but not the voltage, is the operation point in AMOLED applications. Thus, only the drift of  $I_{Semit}$  has influence on the efficiency decay, but not the drift of the serial resistance  $R_{ser}$ .

The reduced current efficiency can be ascribed to the reduced  $I_{Semit}$ . For a constant current  $I_{oled}$ , the voltage across the internal diode voltage  $U_0$  increases. Although other model parameters are modeled as stable/invariant,  $I_{emit}$  is reduced, whereas  $I_{non}$  is increased, so that the sum of both remains constant. The current efficiency is decreased.

To evaluate the degraded  $I_{Semit}$ , the combined data-counting and correlation approaches in Section 5.1 may provide the input, namely, the aging status at a defined medium operation point ( $\eta_{STATUS}$ ). The current distribution between  $I_{emit}$  and  $I_{non}$  at this operation point can be gained by offline simulation of the equivalent circuit, whereas the parameter  $I_{Semit}$  is varied. The relationship between the parameter  $I_{Semit}$  and  $\eta_{STATUS}$  is expected as a monotonic function as expressed in Equation 11. Please note that the ratio between an aged  $I_{Semit}$  and the pristine parameter ( $I_{S_0}$ ) is not equal to the relative efficiency  $\eta_{STATUS}$ . The dependence of the relative efficiency on operation point is a nonlinear function of  $I_{Semit}$ , as the set of Equations 8–10.

$$I_{Semit} = h(\eta_{STATUS}) \quad (11)$$

Simulation of the equivalent circuit may yield to the relative efficiency in dependence on the operation point. For

an operation point  $I_{OLED}$ , the current distribution between  $I_{emit}$  and  $I_{non}$  depends on the saturation current of  $D_{emit}$ , although the sum of both currents is constant ( $I_{OLED}$ ). The ratio between the simulated  $I_{emit}$  for a given  $I_{Semit}$  and the simulated  $I_{emit}$  in the pristine state is equal to the relative efficiency  $\eta_{STATUS}$ . For  $\eta_{STATUS} = 1$ , the parameter  $I_{Semit}$  has the value of  $I_{S_0}$ .

This equivalent circuit allows the simulation over a wide range of operation points. Because the aging status ( $\eta_{STATUS}$ ) is to be considered, the parameter  $I_{Semit}$  will be varied, whereas the operation point in the simulation is the defined operation point for the combined data-counting and correlation models. A relationship between the relative efficiency and this parameter, as Equation 11 indicates, may be established. In a further and more complex simulation run, the parameter  $I_{Semit}$  and the operation point  $I_{OLED}$  are varied. The ratio between the simulated  $I_{emit}$  at an operation ( $I_{OLED}$ ) and for a given  $I_{Semit}$  and the simulated  $I_{emit}$  at the same operation point and for the pristine parameter  $I_{S_0}$  is the effective efficiency in aging process for this OP, as the equation below shows.

$$\begin{aligned} \eta_{EFF} &= \frac{I_{emit}(I_{OLED}, I_{Semit})}{I_{emit}(I_{OLED}, I_{S_0})} = j1(I_{OLED}, I_{Semit}) \\ &= j2(I_{OLED}, \eta_{STATUS}) \end{aligned} \quad (12)$$

By substituting  $I_{Semit}$  in  $j1$  function by  $\eta_{STATUS}$  as the reversal of Equation 11, a function ( $j2$ ) depending on  $I_{OLED}$  and  $\eta_{STATUS}$  can be derived. This function is based on extensive simulation, which is executed in an offline mode. The result is a two-dimensional function with an operation point  $I_{OLED}$  and an aging status  $\eta_{STATUS}$ . The 2D function may be stored in a lookup table (LUT). During the online pixel pipeline processing, the aging status  $\eta_{STATUS}$  can be simply read out from the LUT and used in real-time aging compensation processing. This way, the three approaches, data-counting, correlation, and the electro-optical models, are unified allowing an effective aging compensation.

### 5.3 | Aging compensation for AMOLEDs

OLED aging causes reduced luminance, and differential aging causes image-sticking artifacts. This is the main problem with AMOLEDs. An effective method mitigating this problem is to increase gray value for an aged pixel, so that the luminance objective is met. This is called aging compensation and can be implemented on a control chip, which delivers control signals for an AMOLED panel.

It is described above that the relative efficiency depends on the operation point. For the two principal driving technologies, analog and digital driving, the operation ranges are very different. Although the operation point for digital driving is nearly constant and the gray value is realized by on-time, the operation point for analog driving varies over a wide range of several magnitudes, whereas the lighting time is constant.

This difference between analog and digital driving leads to two different algorithms for the compensation. The base for the compensation is nevertheless the same, namely, the unified OLED aging model with the relative efficiency for an operation point as the output.

### I. Digital driving

For a digital driving system, the gray values are modulated by lighting time. Because the pixels are driven at a constant voltage, the luminance loss is attributed to both current flow and current efficiency. The luminance loss due to current drift could be directly measured by electronic means and compensated.

The compensation of the decay of current efficiency requires an aging model as described in this paper. However, the operation point  $I_{OLED}$  varies in a narrow range. For the determination of the relative efficiency, the operation point may be set as constant. Thus, the effective efficiency  $\eta_{EFF}$  according to Equation 12 is now a one-dimensional function with just one input, the aging status  $\eta_{STATUS}$ .

The aging status  $\eta_{STATUS}$  of every pixel is modeled and calculated according to Section 5.2 and stored in a frame buffer. A gray value for a pixel  $GV_{ORIG}$  is the control signal, which corresponds to a total on-time of the pixel. In the case of an aged pixel,  $\eta_{STATUS}$  and  $\eta_{EFF}$  are below the value 1. The effective efficiency  $\eta_{EFF}$  may be read from a one-dimensional LUT, because the operation point is constant. The input of the 1D LUT is the aging status of this pixel  $\eta_{STATUS}$  and the output  $\eta_{EFF}$ . The equation below will deliver the compensated gray value used to control this pixel.

$$GV_{COMP} = \frac{GV_{orig}}{\eta_{EFF}} \quad (13)$$

$GV_{COMP}$  is the compensated gray value. The on-time, that is, the lighting time of the pixel, is extended. The luminance generated shall be identical to the luminance of an unaged pixel with the  $GV_{ORIG}$  duration.  $GV_{COMP}$  is transmitted to the display controller unit.

For the case that a strongly decreased  $I_{OLED}$  has to be considered or a very high accuracy is required for the compensation, Equation 12 with decayed  $I_{OLED}$  will be

used. The input  $I_{OLED}$  may be approximated from the aging status  $\eta_{STATUS}$  and Equation 3, so that Equation 12 is turned to a different 1D LUT. Compared with digital driving, the compensation for analog driving is more complicated.

### II. Analog driving

For analog driving, the dependence of the efficiency on the operation point is a much more crucial issue.<sup>19</sup> For the original gray value  $GV_{ORIG}$ , there is a corresponding current  $I_{ORIG}$ . This current is not necessarily proportional to the original linear gray value, as the current efficiency is not constant in the pristine state but depends on the operation point.

$$I_{ORIG} = k(GV) \quad (14)$$

$$DATA = D(I_{OLED}) \quad (15)$$

For an OLED current given or a gray value ( $GV$ ) given, there is an LUT for the controlling signal ( $DATA$ ), which is applied to the driver transistor of the pixel circuit. The TFT transistor is operated as an analog current source and feeds a current, for example,  $I_{ORIG}$  into the OLED of the pixel. Due to operational aging, the efficiency is decreased and an effective efficiency  $\eta_{EFF}$  may be obtained from the aging model as described in this paper. The OLED current may be increased to a compensated value  $I_{COMP}$  for which the following equation is valid.

$$I_{COMP} \cdot \eta_{EFF} = I_{COMP} \cdot j2(I_{COMP}, \eta_{STATUS}) = I_{ORIG} \cdot \mathbf{1} \quad (16)$$

The function  $j2$  is that of Equation 12. The equation above is an implicit equation for  $I_{COMP}$  needed to control the pixel circuit, so that the image-sticking artifacts can be compensated. Common methods solving this equation may be applied. One is binary search that has a limited complexity and can be executed within a defined number of processor clocks.

Figure 15 shows a procedure to calculate  $I_{COMP}$  and provides the control signal  $DATA$ . The input gray value for a pixel leads to a current  $I_{ORIG}$  by reading a 1D LUT  $k$  ( $GV$ ), whereas the aging status of the pixel  $\eta_{STATUS}$  can be read out from a memory for aging status. The SOLVER module may iteratively solve Equation 16. One method is a binary search method. An  $I_{COMP}$  may be approximated and fed to  $j2$  2D LUT for  $\eta_{EFF}$ , whereas  $\eta_{STATUS}$  is the other input of this 2D LUT. The distance between the product of the output and of the 2D LUT,  $\eta_{EFF}$  and approximated  $I_{COMP}$ , and  $I_{ORIG}$  is checked against

Equation 16. In the event the product is too low,  $I_{COMP}$  is increased at a defined bit position. Otherwise,  $I_{COMP}$  is decreased at a defined bit position. The bit position starts from the most significant bit (MSB) and will be subsequently moved to a lower position till the least significant bit (LSB). This way, the number of iterations is limited, and the final distance shall be sufficiently small. The output of SOLVER is  $I_{COMP}$ , which leads to a DATA signal controlling the pixel circuit.

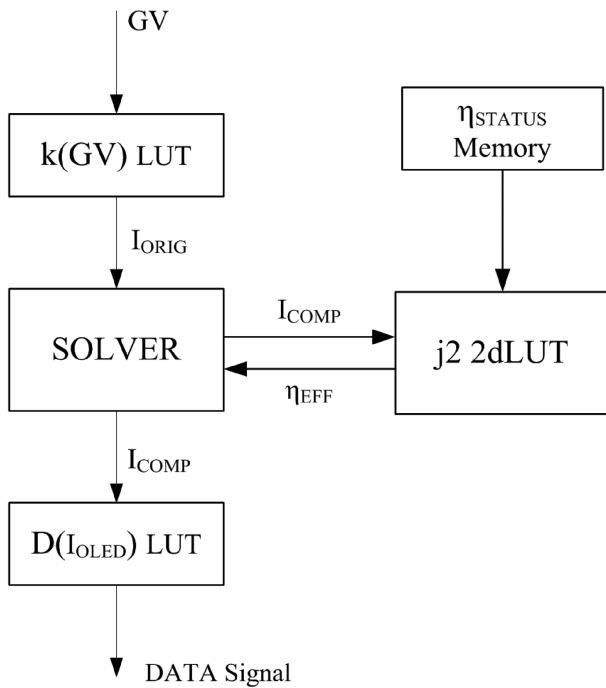


FIGURE 15 Aging compensation procedure for analog driving

Thus, the unified OLED aging model as described in this paper provides an accurate and efficient method to suppress the scared image-sticking artifact for analog driving scheme as well as for digital driving scheme. Overall, the key of the aging compensation is the quality of the aging model.

An aging compensation method has been applied for a digital driving AMOLED display.<sup>18</sup> A test image was displayed on the panel with and without aging compensation, as Figure 16 shows. The left photo shows image-sticking artifacts marked by the two yellow bubbles. With compensation, the image-sticking artifacts on AMOLED display were alleviated. Thus, the lifetime of AMOLED displays may be extended.

## 6 | SUMMARY

In this paper, three OLED aging models have been analyzed with respect to their strengths and weaknesses, respectively. The data-counting model, which considers the acceleration effects of current amplitude and temperature, is accurate in the beginning aging phase. It is a look-forward method and can deliver aging status online. The correlation model in the beginning aging phase is less dependable due to the asynchronous electrical and optical decay. In a more aged state, an effect of the decreasing radiative quantum efficiency by traps in emission layer dominates the degradation. A high correlation between relative current drift, which is measurable, and relative efficient drift may be established. This feedback method may calibrate the data-counting model so that the strengths of these two models are combined.

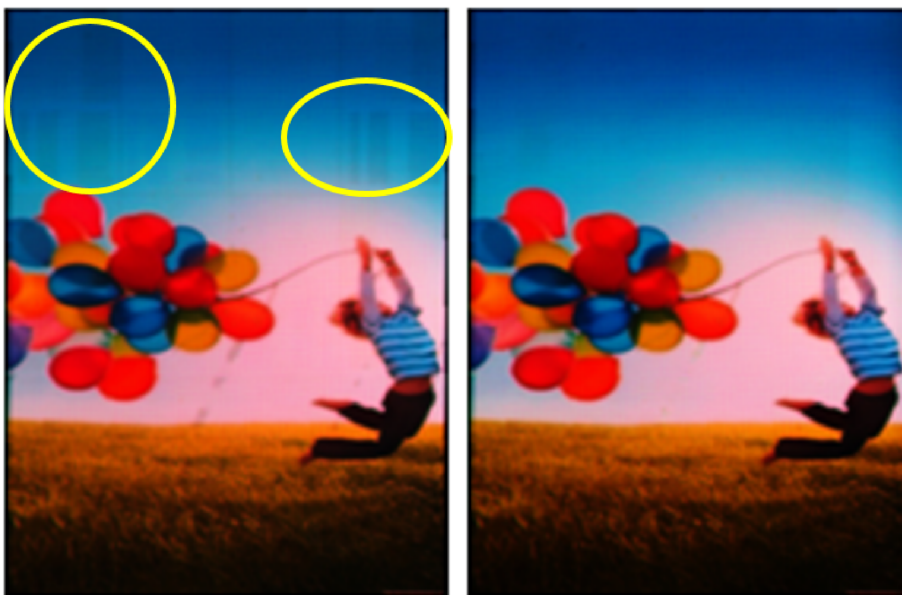


FIGURE 16 A test image displayed without (left) and with aging applying compensation (right) on a digital driving AMOLED

The electro-optical model with an equivalent circuit is the third model considered in this paper. It describes the dependence of the current efficiency on the operation point. The drifting parameter is mainly the saturation current of the emissive diode, which gets smaller with the radiative quantum efficiency decreasing. It has been observed that after a short aging period, the rising serial resistance contributes to the electrical I-V drift, rather than deterioration of the serial interface for serial layers. Whereas the combined model can predict the relative efficiency for one defined operation point, the simulation of the equivalent circuit can deliver relative efficiency as a complex function of the aging status, which is described by the combined model, and the operation point. Thus, the three modeling approaches are unified to one aging model applicable to aging compensation in real display application.

Particularly for analog driving, the operation point lies in a wide range of several magnitudes. A proprietary algorithm for aging compensation has been developed, which may be integrated in pixel pipeline processing. A real-time video operation is practical at a modest processor complexity. With this unified model, a reasonable accuracy within a very long operation time may be expected, so that a significantly longer AMOLED lifetime can be achieved. Moreover, further applications with higher temperature, high brightness, or long lifetime requirements such as automotive and high dynamic range (HDR) may get feasible with AMOLED.

## ACKNOWLEDGMENTS

The authors wish to thank Merck KGaA and Novaled AG for providing OLED device samples. This project is funded by the German Research Foundation (DFG 282450530).

## ORCID

Xingtong Jiang  <https://orcid.org/0000-0002-7036-5705>

## REFERENCES

- Antonio-Torres P, Lister PF, Newbury P. LUT-based compensation model for OLED degradation. *J Soc Inf Disp*. 2005;13(5): 435–441.
- Lee KY, Hsu YP, Chao PCP, Chen WD. A new compensation method for emission degradation in an AMOLED display via an external algorithm, new pixel circuit, and models of prior measurements. *IEEE/OSA J Disp Technol*. 2014;10(3): 189–197.
- Lam HM, Qiu H, Li C, et al. Fast progressive compensation method for externally compensated AMOLED displays. *IEEE J Electron Devices Soc*. 2021;9:257–264.
- Scholz S, Kondakov D, Lüssem B, Leo K. Degradation mechanisms and reactions in organic light-emitting devices. *Chem Rev*. 2015;115(16):8449–8503.
- So F, Kondakov D. Degradation mechanisms in small-molecule and polymer organic light-emitting diodes. *Adv Mater*. 2010; 22(34):3762–3777.
- Schmidt TD, Jäger L, Noguchi Y, Ishii H, Brütting W. Analyzing degradation effects of organic light-emitting diodes via transient optical and electrical measurements. *J Appl Phys*. 2015;117(21):215502.
- Jiang X. Modeling of OLED degradation for prediction and compensation of AMOLED aging artifacts. Dissertation. Saarland University. 2018.
- Kim H, Kim S, Hong Y. Frequency dependency of multi-layer OLED current density-voltage shift and its application to digitally-driven AMOLED. *J Opt Soc Korea*. 2012;16(2): 181–184.
- Jiang X, Volkert P, Xu C. Degradation behavior of blue OLEDs. *SID Symp Dig Tech Pap*. 2015;46(S1):62–62.
- Jiang X, Xu C. Data-counting model for empirical prediction of OLED degradation. *Proc IDW*. 2016. OLED1-3
- Jiang X, Xu C. An electro-optical OLED model for prediction and compensation of AMOLED aging artifacts. *SID Symp Dig Tech Pap*. 2018;49(1):441–444.
- Van Slyke SA, Chen CH, Tang CW. Organic electroluminescent devices with improved stability. *Appl Phys Lett*. 1996;69 (15):2160–2162.
- Parker ID, Cao Y, Yang CY. Lifetime and degradation effects in polymer light-emitting diodes. *J Appl Phys*. 1999;85(4): 2441–2447.
- Soh KM, Xu C, Hitzelberger C. Dependence of OLED display degradation on driving conditions. *Proc SID Mid Eur Chapter Fall Meet*. 2006.
- Giebink NC, Forrest SR. Quantum efficiency roll-off at high brightness in fluorescent and phosphorescent organic light emitting diodes. *Phys Rev B, APS*. 2008;77(23):1–9.
- Chen X, Liu B, Chen Y, Zhao M, Xue CJ, Guo X. Active compensation technique for the thin-film transistor variations and OLED aging of mobile device displays. *IEEE/ACM Int Conf Comput des Dig Tech Pap ICCAD*. 2012;1:516–522.
- Weon BM, Kim SY, Lee JL, Je JH. Evolution of luminance by voltage in organic light-emitting diodes. *Appl Phys Lett*. 2006; 88(1):1–4.
- Volkert P, Jiang X, Xu C. Characterization and compensation of OLED aging in a digital AMOLED system. *J Soc Inf Disp*. 2015;23(12):570–579.
- Xu C, Volkert P. Active matrix organic light-emitting display device and method for driving the same. United States Patent. US10497300. 2016.

## AUTHOR BIOGRAPHIES



**Xingtong Jiang** received his B.E. and M.E. degrees from Xidian University and Xi'an Microelectronics Technology Institute of China, in 2009 and 2013, respectively. In 2019, he was awarded the Doctor of Engineering degree in electrical and electronic engineering with magna cum laude from Saarland University, Germany. Currently, he works as



a postdoc researcher in the Institute of Microelectronics, Saarland University. His research interest is the information display, including the technology of OLED, AMOLEDs, and Driving system.



**Chihao Xu** received his Dipl.-Ing. and Dr.-Ing. degrees in electrical and electronic engineering from Technical University of Munich, Germany, in 1986 and 1990, respectively. From 1986 to 1990, he worked as a research assistant at Technical University of Munich on modeling of power semiconductor devices. From 1991 to 2003, he worked as R&D engineer and R&D manager with Robert Bosch, Infineon Technologies and Dialog Semiconductor, Germany. During this period, he was active in the

research and design of high-voltage integrated circuits for automotive and mobile applications. Since October 2003, he has been the chair professor for microelectronics at Saarland University, Germany. His research focus is in the field of display image processing. It includes addressing and driving schemes for PMOLEDs, local dimming of LED backlights for LCDs, and digital driving for AMOLEDs.

**How to cite this article:** Jiang X, Xu C. A unified OLED aging model combining three modeling approaches for extending AMOLED lifetime. *J Soc Inf Display*. 2021;29:768–784. <https://doi.org/10.1002/jsid.1064>